Radiation pattern in homogeneous and transversely isotropic attenuating media

Satish Sinha*, Sergey Abaseyev and Evgeni Chesnokov****

**Rajiv Gandhi Institute of Petroleum Technology, Rae Bareli, UP 229010 INDIA*

***Department of Earth and Atmospheric Sciences, University of Houston, Houston, TX 77004 USA*

Abstract

Recent advances in shale gas production technologies have compelled exploration and reservoir geophysicists to model seismic characteristics of shales from the fundamental understanding of elastic wave propagation in anisotropic and attenuating media. Shales are anisotropic in nature because of compositional or mineralogical layering within the rocks. Hydraulic fracturing of shales alter the rock properties by inducing fractures and filling them with fluids, thus, changing their attenuation characteristics. Effects of attenuation on the amplitudes of P- and S-waves in vertically transverse isotropic (VTI) media are investigated via radiation patterns. Elastic properties of Barnett shale is used for the modeling purposes. Full waveform synthetic seismograms are generated for various values of attenuation parameter Q assigned to VTI shale. Though Q can be different for P- and S-waves, in this work, same value of Q is assigned to P- and S-waves. Radiation patterns of P- and S-waves suggest that in highly attenuating media, P-wave radiation energy can become comparable to the S-wave radiation energy and in some cases P-wave energy can even be higher than the S-wave energy.

Introduction

Massive scale hydraulic fracture stimulation is common to all shale gas reservoirs being currently produced. Microseismic monitoring method is used to delineate the extent of hydraulic fracturing by installing multicomponent geophones either in the boreholes or on the surface (Maxwell, 2011; Eisner et al., 2011; Abaseyev et al., 2009; Vikhoreva et al., 2011). Huge amount of liquid along with proppant is injected into these low-permeability reservoirs to create permeable pathsways for the gases to flow. Injection of fluids into a reservoir in such a case is expected to change its viscoelastic properties. Highly fractured area of the reservoir would become more attenuating compared to its less fractured or unstimulated part of the reservoir. Shales in horizontally stratified layers are usually anistropic with vertical axis of symmetry known as Vertical Transverse Isotropy (VTI) type. It is due to layering of the clay minerals within the shales. Anisotropic parameters for various shales are listed in Thomsen (1986). When these VTI shales are fractured, one would expect its anisotropic behavior to change depending upon orderliness in the fractures. However, for simplicity, in this work we consider shales to be transversely isotropic and study the effects of attenuation on amplitude characteristics of P- and S-waves by constructing radiation patterns. Such radiation patterns allow us to investigate the focusing of energy in anisotropic attenuating media. Gajewski (1993) and Tsvankin and Chesnokov (1990) constructed radiation patterns in elastic anisotropic media by the ray theory approach and the full waveform theory approach, respectively. Zhu and Tsvankin (2006) studied plane wave propagation in attenuating VTI media. However, they have not shown the effects of attenuation on the classical "butterfly" radiation patterns of dislocation source models. We have used VTI elastic constants from Barnett shale to construct radiation patterns.

Attenuation in a medium is included as a quality factor (Q) as below (White, 1965):

$$C^{*}_{ijkl} = C_{ijkl} + i\,\frac{C_{ijkl}}{Q} \qquad (1)$$

where C_{ijkl} is a fourth rank elasticity tensor. In general, Q can be anisotropic, however, we have assigned same values of Q to P- and S-waves in order to investigate amplitude attenuation with respect to Q. Using spectral-ratio method, Eaton (2011) obtained attenuation parameters for P- and S-waves from microseismic data in Canadian shales.

Methodology

Plane wave propagation in an anisotropic medium is described by the Green-Christoffel equation (Musgrave, 1970).

$$(\Gamma_{ik} - \rho v^2 \delta_{ik}) u_k = 0 \qquad (2)$$

where $\Gamma_{ik} = C_{ijkl} n_j n_L \rho$ is the density and u_k is the displacement (polarization) vector. C_{ijkl} is a fourth rank tensor for the elastic constants and n_j and n_l are direction cosines.

The above system of homogeneous linear equations has a non-trivial solution for the polarization vector

u_k if and only if the matrix G_{ik} of the system has a vanishing determinant:

$$\det(G_{ik}) = \left| a_{ijkl} p_j p_l - \delta_{ik} \right| = 0 \qquad (3)$$

where a_{ijkl} is the density normalized elasticity tensor. Equations resulting from the solution of the Green-Christoffel equation can be found in (Rokhlin and Wang, 2002). Numerical solutions to these equations have instability caused by the acoustic axes in the medium. However, it can be avoided using the perturbation approach. A numerically more stable algorithm can be formed with Stroh Formalism (Stroh, 1962) to compute slowness and polarizations in general anisotropic media.

Stroh Formalism can be written as follows:

$$\partial_z \begin{pmatrix} \mathbf{U} \\ \tau \end{pmatrix} = i\omega \begin{pmatrix} \mathbf{M} & \mathbf{N} \\ -\mathbf{Q} & \mathbf{M}^T \end{pmatrix} \begin{pmatrix} \mathbf{U} \\ \tau \end{pmatrix} \qquad (4)$$

where **U** and τ are displacement and traction vectors, respectively. **M, N,** and **Q** are matrices formulated in Appendix.

Equation (4) is a set of linear differential equations which has the form:

$$\partial_z \mathbf{b}(z) = i\omega \mathbf{A}(z) \mathbf{b}(z) \qquad (5)$$

where **b** is a displacement-traction vector and **A** is called the system matrix of sextic (6x6) form parameterized by elastic constants C_{ijkl}, density and horizontal slownesses.

To compute vertical slowness in a medium with arbitrary symmetry, the Stroh formalism is preferred over the polynomial solution of the Green-Christoffel equation. However, in order to have better accuracy, it is desired to compute the partial derivatives of Green's tensor using polynomial formation of the Green-Christoffel equation. Therefore, a combined method gives a numerically more robust technique for plane wave propagation in anisotropic media.

Radiation Pattern in Isotropic Medium

Seismograms have signatures of both the source and the medium. They are the combined results of source radiation and propagation effects through the media. Therefore, it is important to understand the radiation patterns of various wave types. Figure 1 shows P- and S-wave radiation patterns in a plane containing the vertical force in an unbounded homogeneous isotropic medium (Aki and Richards, 2002).

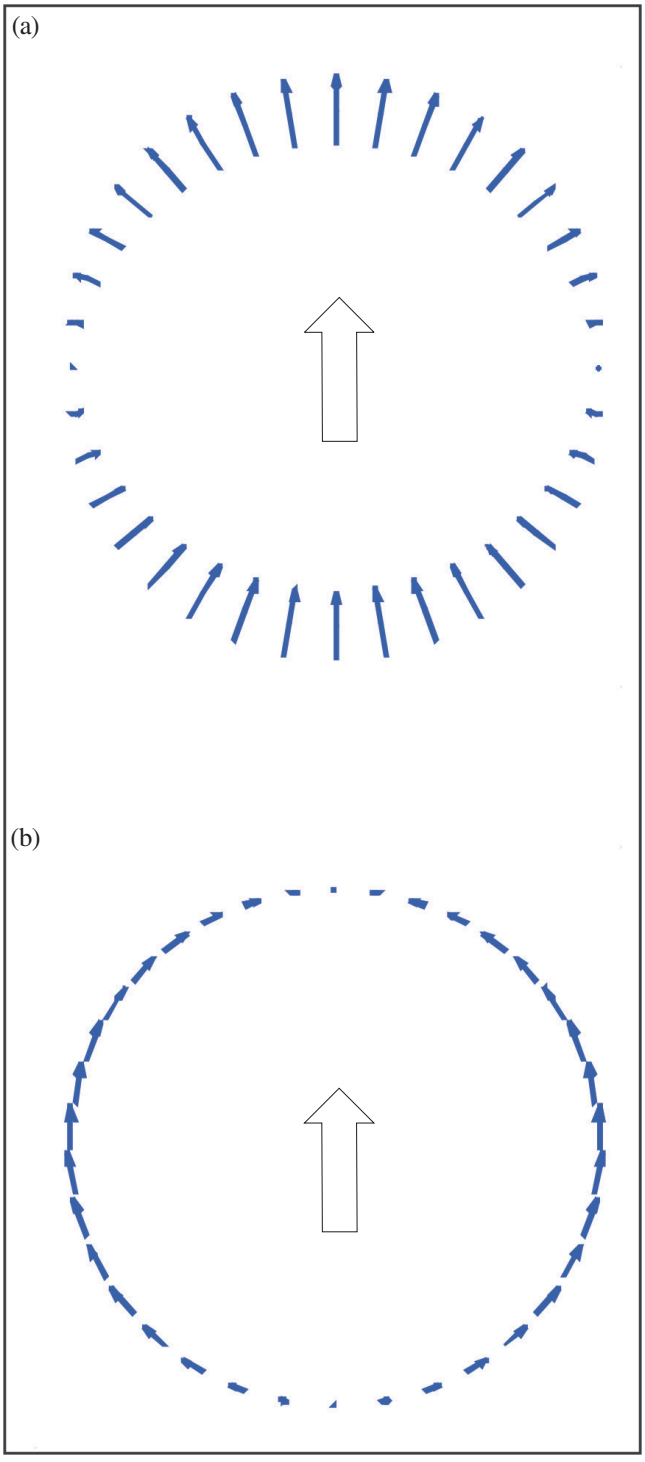

Fig. 1: (a) P-wave radiation pattern (b) S-wave radiation pattern in isotropic media. Arrows at the centers indicate the direction of force.

Important points to note here are:

- Polarization directions are shown by the arrows. P-waves are polarized in the direction of wave propagation, and S-waves are polarized transversely to it.
- P-wave has zero amplitude in the horizontal plane and maximum in the vertical direction.
- S-wave has zero amplitude in the vertical direction and maximum in the X-direction.

- Vertical components of P-wave polarizations in the upper half space are outward, whereas they are inward in the lower half space. Horizontal components are always away from the source.
- Vertical components of S-wave polarizations are in the direction of the applied force and horizontal components are inward in the upper half-space and outward in the lower half-space.
- Horizontal components of P- and S-waves are polarized in opposite directions, whereas their vertical components are polarized in the same direction.

Radiation Pattern in Anisotropic Medium

Now we investigate the radiation patterns in an unbounded homogeneous VTI medium. We have used elastic parameters of Barnett shale in this study. The five independent elastic coefficients and density of this medium are: C_{11} = 21.26, C_{33} = 17.63, C_{44} = 5.32, C_{66} = 8.99, C_{13} = 6.97 GPa and ρ = 2.34 g/cc. The phase velocity characteristics of P-, SH- and SV-waves in the medium are shown in Figure 2.

Full waveform synthetic seismograms are recorded in a vertical plane at receiver placed at 1 km radius from a vertical point source. The frames of 3-component receivers are oriented just as the standard Cartesian system is, with radial, transverse and vertical components being along the X-, Y-, and Z-axis, respectively. Arrival times of P- and S-waves are recorded and plotted radially such as Figure 3. Such plots have radii in temporal units and are in the vertical plane (X-Z plane) containing all the receivers. If such a plot were to be made for an isotropic medium, it would have a constant arrival time forming a quarter circle. In anisotropic medium the arrival times of P- and S-waves do not conform to circles. P-wave arrives before S-waves. Deviation of the color from the background indicates polarity of the waves and intensity of the color is indicative of wave amplitude. Since, the point force vector is along the Z-direction, it produces displacement in vertical and radial directions only, and there is no transverse component of the displacement. Displacement components are shown in the X-Z plane. Note that the radial components of P- and SV-waves are polarized in the opposite direction, whereas vertical components are in the same direction. Displacement amplitude is also consistent with the observation made in the isotropic case.

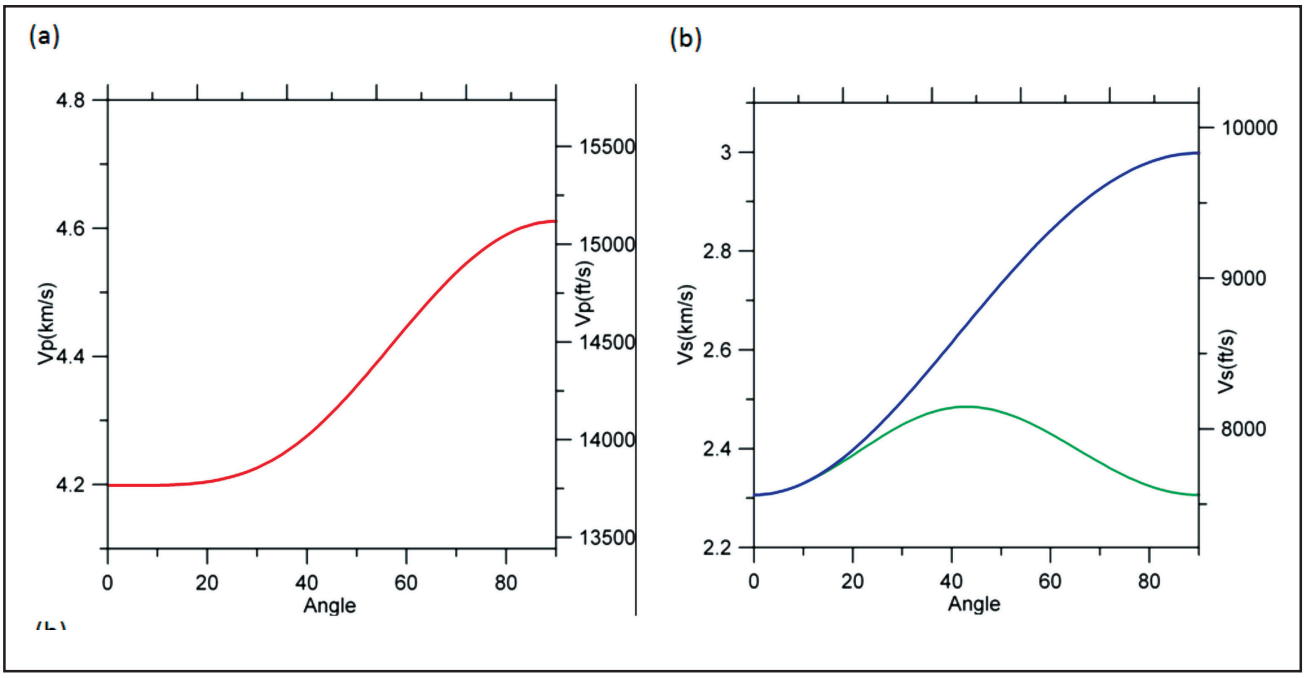

Fig. 2: Phase velocity variation with angle for P-wave is shown in (a), and SV(Green) and SH(Blue) waves are shown in (b).

Effects of Attenuation on P and S Amplitudes

The quality factor (Q) is a measure of attenuation property of a rock and is defined as the quantity proportional to the ratio of the real and imaginary part of elastic coefficients (White, 1965). It essentially represents a viscoelastic medium. Low value of Q suggests a high attenuating medium and vice-versa. The Barnett shale (VTI model) is further analyzed after incorporating various values of Q. Here, radiation patterns are constructed as a polar diagram by taking the

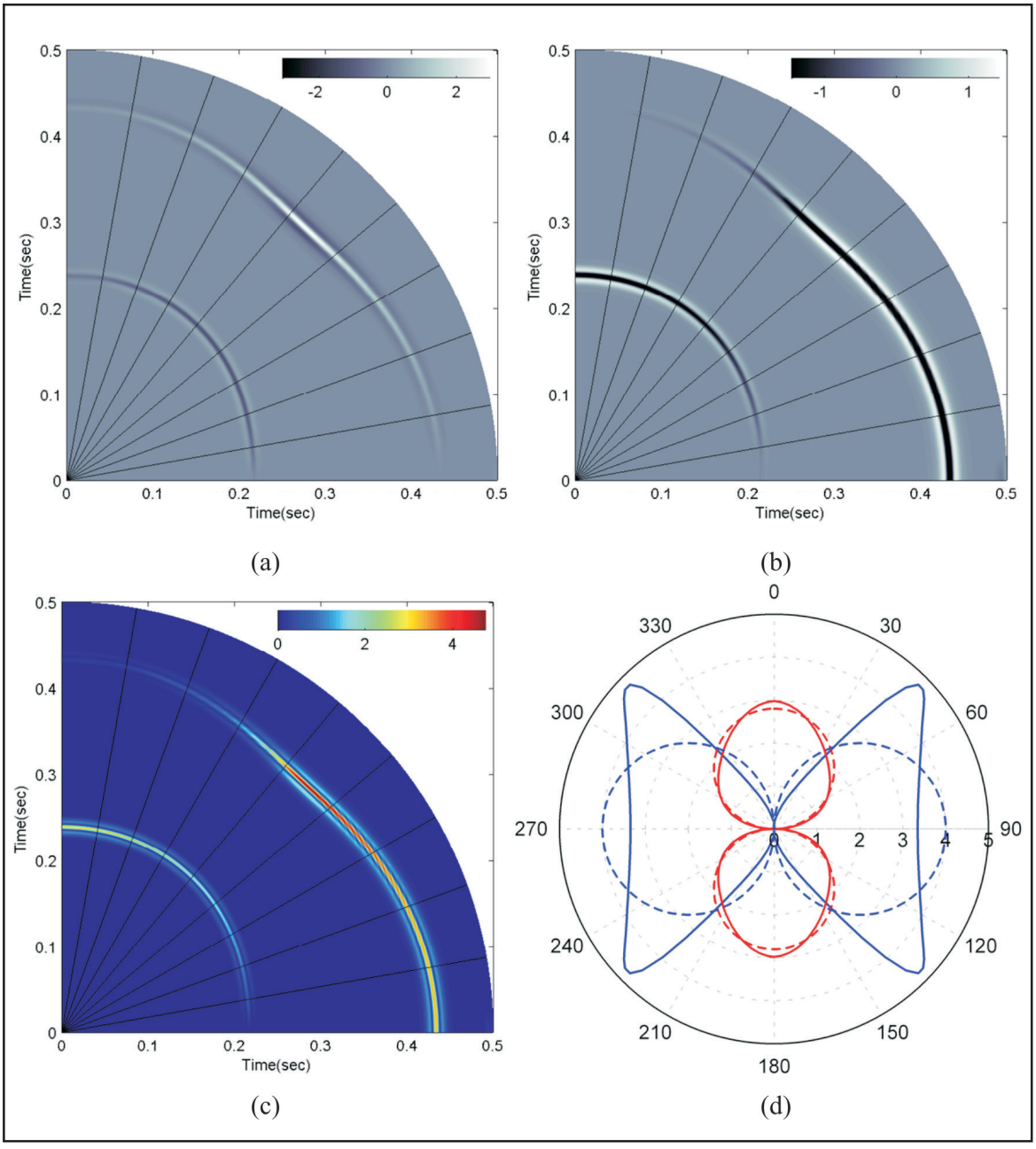

Fig. 3: X- and Z-components of the synthetic seismograms are shown in (a) and (b), respectively. Absolute value of the displacement amplitude is shown in (c). Radiation patterns of P- and S-waves are shown in (d) with red and blue color, respectively. A dashed line represents radiation patterns in an equivalent isotropic medium. Note that the synthetic seismograms are shown only in the first quarter whereas the radiation patterns are shown in all four quarters.

maximum amplitude of the first motions of P- and S-waves in a given plane (vertical plane is shown in our case). The radiation pattern can also be thought of as a far-field radiation in terms of amplitude of the displacement. In order to show the effect of anisotropy, the radiation pattern of an equivalent isotropic medium by a dashed line in Figure 3d. In Figure 4 radiation patterns are shown for Q equal to 1000, 100, 50 and 10 in that order. Radiation patterns appear as a "butterfly" with the head and tail showing P-wave radiation patterns and wings representing S-wave radiation patterns. Note that P-wave radiation shrinks as we increase the quality factor. In each radiation pattern the data are normalized to S-wave maximum amplitude. Change in amplitude can be summarized in a graph plotted in Figure 5. Amplitudes of P- and S-waves both decrease as we decrease the quality factor. Generally, an S-wave has higher amplitude compared to that of a P-wave. Following a critical point on the attenuation axis the P-wave amplitude becomes larger than the S-wave amplitude, while in the radiation pattern "head and tail" becomes larger than the "wings".

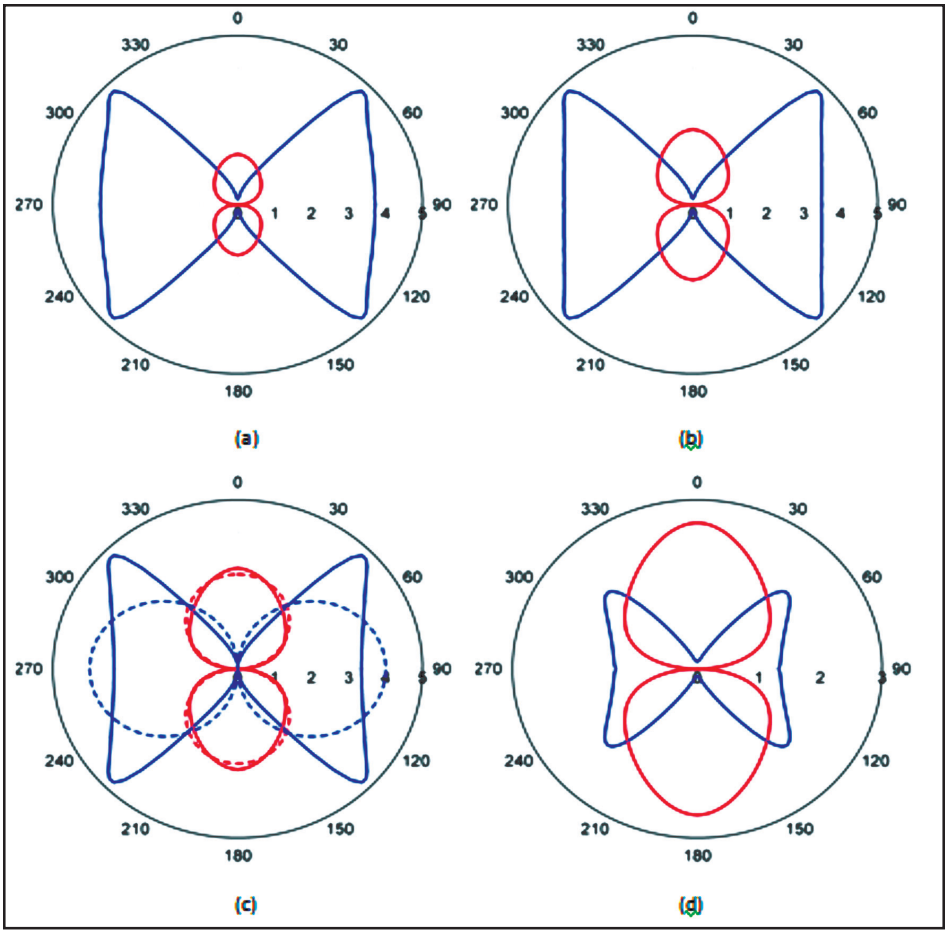

Fig. 4: Radiation patterns are plotted for varying attenuation parameter (Q). (a) Q = 1000 (b) Q = 100 (c) Q = 50 and (d) Q = 10. Radiation patterns of P- and S-waves are shown in (d) with red and blue color, respectively.

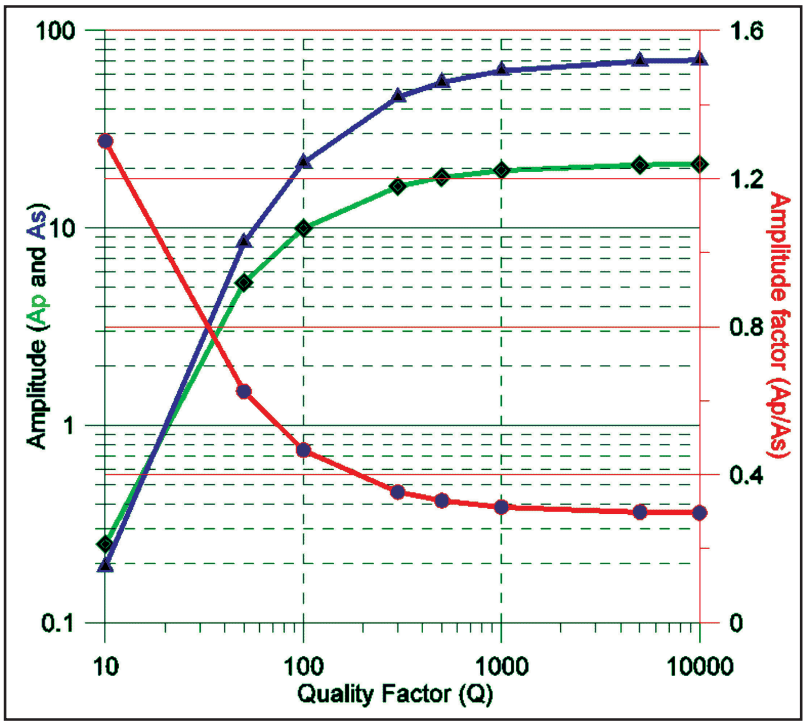

Fig. 5: Change in P- and S-wave amplitudes with respect to quality factor. Amplitude factor is the ratio of P- and S-wave amplitudes.

Discussion and Conclusions

Incorporating P- and S-wave amplitudes variation simultaneously adds another dimension to attenuation studies. Focusing of energy in different orientation along with attenuation in a VTI medium is shown via radiation patterns.

Analysis of P- and S-wave attenuation from seismic data can be useful in reservoir geophysics. In case of a shale gas reservoir, microseismic data associated with hydraulic fracturing are commonly acquired. Some ray paths go through the fractured part of the reservoir and others through unfractured part of the reservoir. Such studies can help delineating the extent of fracturing. This approach can also be useful in heavy oil studies.

Acknowledgements

We are grateful to Devon Energy Inc. and Institute for Theoretical Geophysics to support this study. We also wish to thank Dr. Ray Brown for many useful discussions.

References

Abaseyev, S. S., M. Ammerman, and E. M. Chesnokov, 2009, Automated detection and location of hydrofracking-induced microseismic event from 3 observations in an offsetting monitor well: 79th Ann. Internat. Mtg., Soc. Expl. Geophys., Expanded Abstracts, 1514-1518.

Aki, K. and P. G. Richards, 2002, Quantitative seismology: Univ. Sci. Books.

Eaton, D. W., 2011, Q determination, corner frequency and spectral characteristics of microseismicity induced by hydraulic fracturing: 81st Ann. Internat. Mtg., Soc. Expl. Geophys., Expanded Abstracts, 1555-1559.

Eisner, L., Y. Zhang, P. Duncan, M. C. Mueller, M. P. Thornton, and D. Gei, 2011, Effective VTI anisotropy for consistent monitoring of microseismic events: The Leading Edge, **30**.

Gajewski, D., 1993, Radiation from point sources in general anisotropic media: Geophys. J. Int., **113**, 299-317.

Maxwell, S., 2011, Microseismic hydraulic fracture imaging: The path toward optimizing shale gas production: The Leading Edge, **30**.

Musgrave, M. J. P., 1970, Crystal acoustics: Holden-Day: San Francisco.

Rokhlin, S. I. and L. Wang, 2002, Stable recursive algorithm for elastic wave propagation in layered anisotropic media: Stiffness matrix method: J. Acoust. Soc. Am., **112**, 822-834.

Stroh, A. N., 1962, Steady state problems in anisotropic elasticity: J. Math. Phys., **41**, 77-103.

Thomsen, L., 1986, Weak elastic anisotropy: Geophysics, **51**, 1954-1966.

Tsvankin, I. D. and E. M. Chesnokov, 1990, Synthesis of body wave seismograms from point sources in anisotropic media: J. Geophys. Res., **95**, 11317-11331.

Vikhoreva, A. A., E. M. Chesnokov, M. A. Krasnova, and L. Kuo, 2011, The automatic detection of arrival times of longitudinal and shear waves: 81st Ann. Internat. Mtg., Soc. Expl. Geophys., Expanded Abstracts, 1576-1579.

White, J. E., 1965, Seismic waves: Radiation, transmission, and attenuation. McGraw-Hill Book Co.,Inc., New York.

Zhu, Y. and I. Tsvankin, 2006, Plane-wave propagation in attenuative transversely isotropic media: Geophysics, **71**, T17-T30.

APPENDIX A

STROH FORMALISM

Newton's second law of motion in continuum mechanics can be written as:

$$C_{ijkl}\partial_j\partial_l u_k = \rho\partial_t^2 u_i \tag{A-1}$$

For wave propagation in a layered medium, the displacements and traction are assumed to be continuous throughout the multilayered medium, including its interfaces. The traction vector at a unit plane area parallel to a layer interface is σ_{i3} and can be written as:

$$\sigma_{i3} = C_{i3kl}\partial_l u_k \tag{A-2}$$

$$\text{or, } \sigma_{i3} = \begin{pmatrix} E_x^{ik}\partial_x & E_y^{ik}\partial_y & E_z^{ik}\partial_z \end{pmatrix} \begin{pmatrix} u_x \\ u_y \\ u_z \end{pmatrix} \tag{A-3}$$

where

$$\mathbf{E}_x = E_x^{ik} = C_{i3k1},\ \mathbf{E}_y = E_y^{ik} = C_{i3k2},\ \text{and}\ \mathbf{E}_z = E_z^{ik} = C_{i3k3} \tag{A-4}$$

The displacement and traction vector in the form of a plane wave can be expressed as:

$$\sigma_{i3} = T_i \exp\left[-i\omega\left(p_x x + p_y y - t\right)\right] \tag{A-5}$$

$$u_i = U_i \exp\left[-i\omega\left(p_x x + p_y y - t\right)\right] \tag{A-6}$$

where p_i's are slownesses in the Cartesian coordinates. Substituting equations (A-5) and (A-6) into equation (A-3), one obtains:

$$\begin{pmatrix} T_x \\ T_y \\ T_z \end{pmatrix} = -i\omega\left(p_x\mathbf{E}_x + p_y\mathbf{E}_y\right)\begin{pmatrix} U_x \\ U_y \\ U_z \end{pmatrix} + \mathbf{E}_z\partial_z\begin{pmatrix} U_x \\ U_y \\ U_z \end{pmatrix} \tag{A-7}$$

$$\text{or, } \partial_z\begin{pmatrix} U_x \\ U_y \\ U_z \end{pmatrix} = i\omega\mathbf{E}_z^{-1}\left[\left(p_x E_x + p_y\mathbf{E}_y\right)\right]\begin{pmatrix} U_x \\ U_y \\ U_z \end{pmatrix} + \mathbf{E}_z^{-1}\begin{pmatrix} T_x \\ T_y \\ T_z \end{pmatrix} \tag{A-8}$$

$$\text{or, } \mathbf{U}_{,\mathbf{z}} = i\omega\mathbf{E}_z^{-1}\left[\left(p_x\mathbf{E}_x + p_y\mathbf{E}_y\right)\right]\mathbf{U} + \mathbf{E}_z^{-1}\mathbf{T} \tag{A-9}$$

$$\text{or, } \mathbf{U}_{,\mathbf{z}} = i\omega\mathbf{M}\,\mathbf{U} + \mathbf{N}\,\mathbf{T} \tag{A-10}$$

where $\mathbf{M} = \mathbf{E}_z^{-1}\left[\left(p_x\mathbf{E}_x + p_y\mathbf{E}_y\right)\right]$ and $\mathbf{N} = \mathbf{E}_z^{-1}$.

Now let us look at equation (A-1). Substituting equation (A-6) into (A-1), one obtains:

$$\omega^2 r\,\mathbf{U} = \omega^2\left(p_x^2 F_{xx}^{ik} + p_y^2 F_{yy}^{ik} + 2p_x p_y F_{xy}^{ik}\right)\mathbf{U} - F_{zz}^{ik}\mathbf{U}_{,zz} + 2iw\left(p_x F_{zx}^{ik} + p_y F_{yz}^{ik}\right)\mathbf{U}_{,z} \tag{A-11}$$

where

$$\left.\begin{aligned} \mathbf{F}_{xx} = F_{xx}^{ik} = C_{i1k1} \\ \mathbf{F}_{yy} = F_{yy}^{ik} = C_{i2k2} \\ \mathbf{F}_{zz} = F_{yy}^{ik} = C_{i3k3} \\ 2\mathbf{F}_{xy} = 2F_{xy}^{ik} = C_{i1k2} + C_{i2k1} \\ 2\mathbf{F}_{yz} = 2F_{yz}^{ik} = C_{i2k3} + C_{i3k2} \\ 2\mathbf{F}_{zx} = 2F_{zx}^{ik} = C_{i3k1} + C_{i1k3} \end{aligned}\right\} \tag{A-12}$$

From equalities in (A-4) and (A-12), we get $2\mathbf{F}_{zx}=\left(\mathbf{E}_x+\mathbf{E}_x^T\right)$, $2\mathbf{F}_{yz}=\left(\mathbf{E}_y+\mathbf{E}_y^T\right)$, and $\mathbf{F}_{zz}=\mathbf{E}_z$. Furthermore, differentiating equation (A-10) with respect to z leads to:

$$\mathbf{U}_{,zz}=i\omega\mathbf{M}\,\mathbf{U}_{,z}+\mathbf{N}\,\mathbf{T}_{,z}=i\omega\mathbf{M}\left(i\omega\mathbf{M}\,\mathbf{U}+\mathbf{N}\,\mathbf{T}\right)+\mathbf{N}\,\mathbf{T}_{,z}=-\,\omega^2\mathbf{M}\,\mathbf{M}\,\mathbf{U}+i\omega\mathbf{M}\,\mathbf{N}\,\mathbf{T}+\mathbf{N}\,\mathbf{T}_{,z} \tag{A-13}$$

Substituting values of **U**,zz and **U**,z in equation (A-11), one obtains:

$$\omega^2\rho\mathbf{U}=\omega^2\left(p_x^2\mathbf{F}_{xx}+p_y^2\mathbf{F}_{yy}+2p_xp_y\mathbf{F}_{xy}\right)\mathbf{U}-\mathbf{F}_{zz}\left(-\,\omega^2\mathbf{M}\,\mathbf{M}\,\mathbf{U}+i\omega\mathbf{M}\,\mathbf{N}\,\mathbf{T}+\mathbf{N}\,\mathbf{T}_{,z}\right)+2i\omega\left(p_x\mathbf{F}_{zx}+p_y\mathbf{F}_{yz}\right)\left(i\omega\,\mathbf{M}\,\mathbf{U}+\mathbf{N}\,\mathbf{T}\right)$$

or, (A-14)

$$\begin{aligned}0=\omega^2&\left[p_x^2\mathbf{F}_{xx}+p_y^2\mathbf{F}_{yy}+2p_xp_y\mathbf{F}_{xy}+\mathbf{F}_{zz}\mathbf{M}\,\mathbf{M}-2\left(p_x\mathbf{F}_{zx}+p_y\mathbf{F}_{yz}\right)\mathbf{M}-\rho\mathbf{I}\right]\mathbf{U}\\&-i\omega\left[\mathbf{F}_{zz}\mathbf{M}\,\mathbf{N}-2\left(p_x\mathbf{F}_{zx}+p_y\mathbf{F}_{yz}\right)\mathbf{N}\right]\mathbf{T}-\mathbf{F}_{zz}\mathbf{N}\,\mathbf{T}_{,z}\end{aligned} \tag{A-15}$$

Some of the terms in the above equation can be expanded as follows:

$$\mathbf{F}_{zz}\mathbf{N}=\mathbf{E}_z\mathbf{E}_z^{-1}=\mathbf{I} \tag{A-16}$$

$$\mathbf{F}_{zz}\mathbf{M}\mathbf{M}=\mathbf{E}_z\mathbf{E}_z^{-1}\left(p_x\mathbf{E}_x+p_y\mathbf{E}_y\right)\mathbf{E}_z^{-1}\left(p_x\mathbf{E}_x+p_y\mathbf{E}_y\right)=\left(p_x\mathbf{E}_x+p_y\mathbf{E}_y\right)\mathbf{E}_z^{-1}\left(p_x\mathbf{E}_x+p_y\mathbf{E}_y\right) \tag{A-17}$$

$$2\left(p_x\mathbf{F}_{zx}+p_y\mathbf{F}_{yz}\right)\mathbf{M}=\left[p_x\left(\mathbf{E}_x+\mathbf{E}_x^T\right)+p_y\left(\mathbf{E}_y+\mathbf{E}_y^T\right)\right]\mathbf{E}_z^{-1}\left(p_x\mathbf{E}_x+p_y\mathbf{E}_y\right)=\mathbf{F}_{zz}\mathbf{M}\mathbf{M}+\left(p_x\mathbf{E}_x^T+p_y\mathbf{E}_y^T\right)\mathbf{E}_z^{-1}\left(p_x\mathbf{E}_x+p_y\mathbf{E}_y\right) \tag{A-18}$$

$$\mathbf{F}_{zz}\mathbf{M}\mathbf{N}=\mathbf{E}_z\mathbf{E}_z^{-1}\left(p_x\mathbf{E}_x+p_y\mathbf{E}_y\right)\mathbf{E}_z^{-1}=\left(p_x\mathbf{E}_x+p_y\mathbf{E}_y\right)\mathbf{E}_z^{-1} \tag{A-19}$$

$$2\left(p_x\mathbf{F}_{zx}+p_y\mathbf{F}_{yz}\right)\mathbf{N}=\left[p_x\left(\mathbf{E}_x+\mathbf{E}_x^T\right)+p_y\left(\mathbf{E}_y+\mathbf{E}_y^T\right)\right]\mathbf{E}_z^{-1}=\mathbf{F}_{zz}\mathbf{M}\mathbf{N}+\left(p_x\mathbf{E}_x^T+p_y\mathbf{E}_y^T\right)\mathbf{E}_z^{-1} \tag{A-20}$$

Substituting equations from (A-16) to (A-20) into equation (A-15), one obtains:

$$\begin{aligned}\mathbf{T}_{,z}=\omega^2&\left[p_x^2\left(\mathbf{F}_{xx}-\mathbf{E}_x^T\mathbf{E}_z^{-1}\mathbf{E}_x\right)+p_y^2\left(\mathbf{F}_{yy}-\mathbf{E}_y^T\mathbf{E}_z^{-1}\mathbf{E}_y\right)+p_xp_y\left(2\mathbf{F}_{xy}-\mathbf{E}_x^T\mathbf{E}_z^{-1}\mathbf{E}_y-\mathbf{E}_y^T\mathbf{E}_z^{-1}\mathbf{E}_x\right)-\rho\mathbf{I}\right]\mathbf{U}\\&+i\omega\left[\left(p_x\mathbf{E}_x^T+p_y\mathbf{E}_y^T\right)\mathbf{E}_z^{-1}\right]\mathbf{T}\end{aligned} \tag{A-21}$$

or, $$\mathbf{T}_{,z}=\omega^2\mathbf{Q}\mathbf{U}+i\omega\mathbf{R}\mathbf{T} \tag{A-22}$$

where

$$\begin{aligned}\mathbf{Q}&=p_x^2\mathbf{Q}_1+p_y^2\mathbf{Q}_2+p_xp_y\mathbf{Q}_3-\rho\mathbf{I}\\\mathbf{Q}_1&=\mathbf{F}_{xx}-\mathbf{E}_x^T\mathbf{E}_z^{-1}\mathbf{E}_x\\\mathbf{Q}_2&=\mathbf{F}_{yy}-\mathbf{E}_y^T\mathbf{E}_z^{-1}\mathbf{E}_y\\\mathbf{Q}_3&=2\mathbf{F}_{xy}-\mathbf{E}_x^T\mathbf{E}_z^{-1}\mathbf{E}_y-\mathbf{E}_y^T\mathbf{E}_z^{-1}\mathbf{E}_x\end{aligned} \tag{A-23}$$

and, $\mathbf{R}=\left(p_x\mathbf{E}_x^T+p_y\mathbf{E}_y^T\right)\mathbf{E}_z^{-1}$

Combining (A-10) and (A-22), one can write:

$$\partial_z\begin{pmatrix}\mathbf{U}\\\boldsymbol{\tau}\end{pmatrix}=i\omega\begin{pmatrix}\mathbf{M}&\mathbf{N}\\-\mathbf{Q}&\mathbf{R}\end{pmatrix}\begin{pmatrix}\mathbf{U}\\\boldsymbol{\tau}\end{pmatrix}=i\omega\begin{pmatrix}\mathbf{M}&\mathbf{N}\\-\mathbf{Q}&\mathbf{M}^T\end{pmatrix}\begin{pmatrix}\mathbf{U}\\\boldsymbol{\tau}\end{pmatrix} \tag{A-24}$$

where $\boldsymbol{\tau}=\mathbf{T}/i\omega$ and $\mathbf{R}=\mathbf{M}^T$